ACCOUNTS of chemical research

Article

pubs.acs.org/accounts

Optics, Mechanics, and Energetics of Two-Dimensional MoS_2 Nanostructures from a Theoretical Perspective

Published as part of the Accounts of Chemical Research special issue "2D Nanomaterials beyond Graphene".

Jan-Ole Joswig,*[,†] Tommy Lorenz,[†,‡] Tsegabirhan Berhane Wendumu,[†,§] Sibylle Gemming,[‡,∥] and Gotthard Seifert[†]

[†]Theoretical Chemistry, Technical University Dresden, 01162 Dresden, Germany

[‡]Institute of Ion Beam Physics and Materials Research, Helmholtz-Zentrum Dresden-Rossendorf e.V., P.O. Box 510119, 01314 Dresden, Germany

[§]Max Planck Institute for the Physics of Complex Systems, 01187 Dresden, Germany

[∥]Theoretical Physics, Faculty of Sciences, Technical University Chemnitz, 09107 Chemnitz, Germany

CONSPECTUS: Nanostructures based on molybdenum disulfide (MoS_2) are by far the most common and well-studied systems among two-dimensional (2D) semiconducting materials. Although still being characterized as a "promising material", catalytic activity of MoS_2 nanostructures has been found, and applications in lubrication processes are pursued. Because exfoliation techniques have improved over the past years, monolayer MoS_2 is easily at hand; thus, experimental studies on its electronic properties and applicability are in scientific focus, and some MoS_2-based electronic devices have been reported already. Additionally, the improvement of atomic force microscopy led to nanoindentation experiments, in which the exceptional mechanical properties of MoS_2 could be confirmed. In this Account, we review recent results from density-functional based calculations on several MoS_2-based nanostructures; we have chosen to follow several experimental routes focusing on different nanostructures and their specific properties.

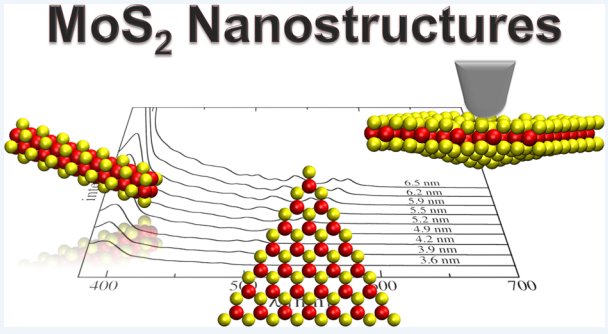

MoS_2-based triangular nanoflakes are systems that are experimentally well described and studied with a special focus on their optical absorption. The interpretation of our calculations fits well to the experimental picture: the absorption peaks in the visible light range show a quantum-confinement effect; they originate from excitations into the edge states. Additionally, delocalized metallic-like states are present close to the Fermi level, which do not contribute to photoabsorption in the visible range.

Additionally, nanoindentation experiments have been simulated to obtain mechanical properties of the MoS_2 material and to study the influence of deformation on the system's electronics. In these molecular-dynamics simulations, a tip penetrates a MoS_2 monolayer, and the obtained Young's modulus and breaking stress agree very well with experimentally obtained values. Whereas the structural properties, such as bond lengths and layer contraction, vary locally differently upon indentation, the electronic structure in terms of the density of states, the gap between occupied and unoccupied states, or the quantum transport change only slightly. The robustness of the material with respect to electronic and mechanical properties makes monolayer MoS_2 special. However, it is important to note that this robustness refers to a local disturbance through deformation and still seems to be dependent on the defect concentration.

Finally, we present a comparison of the thermodynamic stabilities of different MoS_2-based nanostructures with a focus on nanoflakes, fullerene-like nanooctahedra, and smaller Chevrel-type and non-Chevrel-type clusters (nanowires). All studied systems are stable in comparison to MoS_2, Mo bulk, and the S_8 crown, but only the studied nanoflakes and nanowires show specific stoichiometries, either sulfur-rich or sulfur-poor, whereas the nanooctahedra may adopt both. From the thermodynamic stabilities, it should be possible to deliberately choose specific nanostructures by thoughtful choices of the synthesis conditions.

In conclusion, we present in this Account exceptional properties of MoS_2-based nanostructures studied by means of density-functional theory. The focus lies on optical absorption in the visible range observed in triangular nanoflakes, which originate in the system's edge states, the robustness of monolayer MoS_2 with respect to punctual loads regarding both mechanical and electronic properties, and the thermodynamic stability of most studied MoS_2-based nanosystems revealing a correlation between composition and preferred morphology, particularly for 2D systems.

Special Issue: 2D Nanomaterials beyond Graphene

Received: August 27, 2014
Published: December 9, 2014

1. INTRODUCTION

In these days, nanostructures based on two-dimensional transition-metal dichalcogenides are investigated intensively after moving into the focus of research already quite a while ago. Since the 1950s, molybdenum disulfide has been studied with respect to its surface, catalytic, and lubrication properties.[1] At the latest since the Nobel Prize was awarded to Geim and Novoselov in 2010 "for groundbreaking experiments regarding the two-dimensional material graphene", two-dimensional materials other than graphene have been highly pushed as alternatives, among them the long-known and well-studied molybdenum disulfide (MoS_2).

Being structurally and electronically related to $MoSe_2$, WS_2, and WSe_2,[2,3] molybdenum disulfide is one of the most common transition-metal dichalcogenides. It occurs as the mineral molybdenite and exhibits a wealth of characteristic sizes, shapes, and bonding motifs in the nanostructural regime, each with distinct local chemical and electronic properties. Figure 1 depicts parts of an MoS_2 layer in different views and highlights the trigonal prismatic coordination of the molybdenum atoms. On the nanoscale, several types of MoS_2 nanostructures are known: zero-dimensional (0D) clusters ranging from small structures[4−7] to hollow nanoscale octahedra,[8−10] one-dimensionally (1D) extended wires,[11−13] or tubes[14−16] with diameters of the order of nanometers or two-dimensionally extended, flat triangular nanoflakes[1,4,5] and monolayers. Especially the transition region between the different morphologies has been studied extensively by density functional calculations.[5,6,9] Examples of some of the mentioned compounds can be found as insets in most figures of this Account.

In agreement with data from electron microscopy and scanning probe investigations, geometries obtained by density-functional calculations reflect its trilayer structure (three covalently interconnected layers of S, Mo, and S atoms, see Figure 1b) of the unperturbed, stoichiometric MoS_2 sheet in the major part of both nanooctahedra and nanoflakes.[10,17] Deviations occur only along the terminating edge and corner sites, where the composition and atom arrangement differ locally from the situation in the pure two-dimensional bulk. There, one-dimensionally extended electronic states have been detected and discussed as the origin of the specific activity of those compounds as desulfurization catalysts.[1,8]

Similar one-dimensional states have been proposed to occur along the edge termination of molybdenum disulfide nanoribbons.[18] Tubular architectures with perfect MoS_2 composition (not shown here) are obtained by rolling and seamless closure of such nanoribbons. Regardless of the rolling direction, MoS_2 tubes are always semiconducting, with the gap size depending on the diameter, which sets the local curvature.[14,15] Substitutional or interstitial doping of Mo sites by aliovalent transition metals may be employed to induce electronic states within this gap.[16,19]

One-dimensionally extended wires, on the other hand, consist of a metallic core based on molybdenum triangles, and a terminating sulfur shell. Density-functional calculations and scanning tunneling data both indicate metallic conductance along the interior of such nanowires, which can be contacted by gold electrodes and are robust against bending but sensitive to torsion.[6,11,20−23] Sulfur-poor clusters are built from the same structural motif and terminated either by a single sulfur atom (Chevrel-type clusters) or by a less sulfur-poor terminating MoS_4 unit.[6]

Besides the nanostructured systems discussed so far, MoS_2 sheets, that is large quasi-infinite monolayers, can be obtained, for example, from the bulk material by micromechanical cleavage techniques.[24−26] Through new low-cost exfoliation techniques, single layers became accessible. These structures are of special interest for the production of electronic devices, especially because bulk MoS_2 has an indirect band gap of 1.2 eV,[27] which becomes direct in the monolayers due to quantum confinement.[28−31] To date, a number of electronic devices based on MoS_2 have been reported, for example, field-effect transistors, logic circuits, and amplifiers,[32−34] and this field has been reviewed by Kis et al.[35] recently.

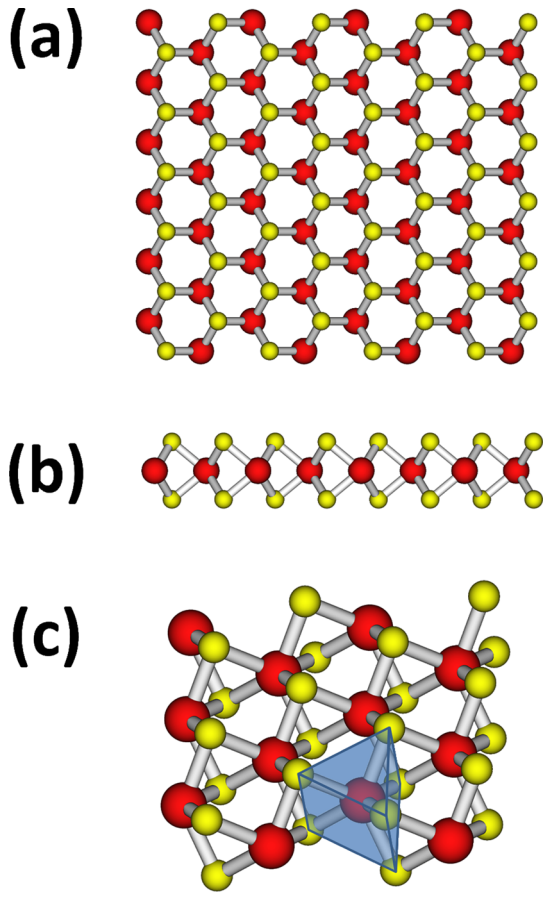

Figure 1. Structures of a molybdenum disulfide monolayer in (a) top view, (b) side view, and (c) oblique view with highlighted trigonal prismatic coordination of a molybdenum atom. The molybdenum and sulfur atoms are represented as red and yellow spheres, respectively.

In addition to the exceptional electronic properties, transition-metal dichalcogenide based materials exhibit a certain robustness upon mechanical stress.[36−39] For example, tensile tests on WS_2 nanotubes show large Young's moduli and rather broad linear strain−stress relations,[40] and MoS_2 layers are predicted to behave likewise.[41] This changes, when the 2D material is globally deformed, for example, under biaxial stress.[42]

This Account summarizes and relates several discussions of optical, mechanical, and energetic properties of MoS_2 nanostructures. All studies were performed using a similar computational approach that will be briefly mentioned in section 2. Afterward, we will discuss the optical absorption spectra of triangular MoS_2 nanoflakes in section 3 and the mechanical and electronic properties of MoS_2 monolayers under deformation in sections 4 and 5. We then will compare the grand canonical stability of MoS_2-based nanostructures in section 6 and finally conclude in section 7.

dx.doi.org/10.1021/ar500318p | Acc. Chem. Res. 2015, 48, 48−55

2. COMPUTATIONAL METHODS

For all calculations, a density-functional[43,44] tight-binding (DFTB) method[45−48] was employed either for single-point calculations, for geometry optimizations, or for Born−Oppenheimer molecular-dynamics simulations; the Slater−Koster integral tables used were described earlier.[49] The optical absorption spectra were calculated using a modified[50] linear response approach by Casida[51,52] implemented in an experimental version of the deMon computer code.[53] The simulated indentation experiment employed the London dispersion correction of Zhechkov et al.[54] For comparison, structural optimizations for the biaxial stretched planar MoS_2 monolayer were performed with the DFTB+ program package.[55,56] For the exact details, we refer the interested reader to the original publications, which are mentioned at the appropriate places.

3. OPTICAL EXCITATIONS IN TRIANGULAR MoS_2 NANOFLAKES

In many cases, nanostructures exhibit the topology of their respective bulk material. Exceptions are those cases, when allotropes are formed: for example, fullerenes are related to the planar graphene structure but form a separate class of nanomaterials. In this sense, nanostructures obtained from layered bulk materials are special, because their bulk topology is conserved in the finite system. Thus, materials like MoS_2 form flakes consisting of a single layer, in which the original topology is conserved except at the edges, where the periodicity is broken. As a consequence of the hexagonal in-plane symmetry of a MoS_2 layer, these flakes have either triangular or rhomb-like shapes. Nanoflakes with zigzag edges are additionally terminated with sulfur atoms so that the true stoichiometry is in fact not 1:2, but these particles are slightly sulfur-rich (see insets of Figure 2). Nevertheless, we will continue addressing them as MoS_2 nanoflakes.

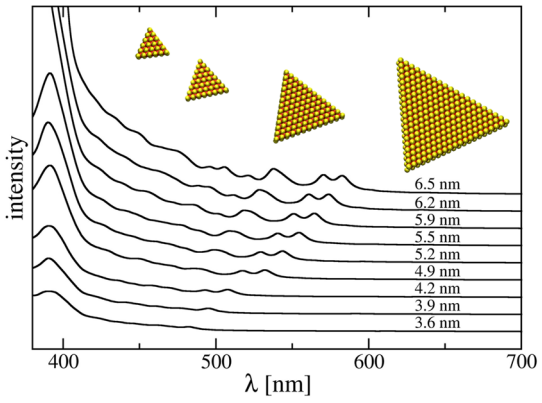

Figure 2. Absorption spectra of zigzag MoS_2 nanoflakes with different sizes calculated with the time-dependent DFTB method. The spectra are labeled according to the different edge lengths, *d*, and shifted in *y* direction for better visibility. Inset: four trigonal MoS_2 nanoflakes with different edge lengths.

Triangular MoS_2 nanoflakes have been studied experimentally and theoretically in detail already.[4,5,17,31] We will add some new aspects here from a very recent study of the optical absorption in such nanoflakes.[57] Figure 2 displays the calculated optical absorption spectra of triangular MoS_2 nanoflakes in the visible range of the electromagnetic spectrum. With increasing edge length, *d*, the absorption peaks are red-shifted, which illustrates the quantum confinement in such systems. The covered range of the low-energy absorption is 480 to 580 nm. This corresponds to energies of 2.6 to 2.2 eV. The corresponding excitation energy in bulk MoS_2 is at 650 nm (1.9 eV). These excitations agree with the experimental data[58,59] and fit very well to the Brus equation,[60] that is, the energy of the absorption in the visible light region follows a $1/d^2$ behavior for particles larger than ∼3 nm and converges asymptotically to the bulk value (1.9 eV).

A further analysis of the density of states and its projection on the molybdenum atoms in Figure 3 illustrates the special

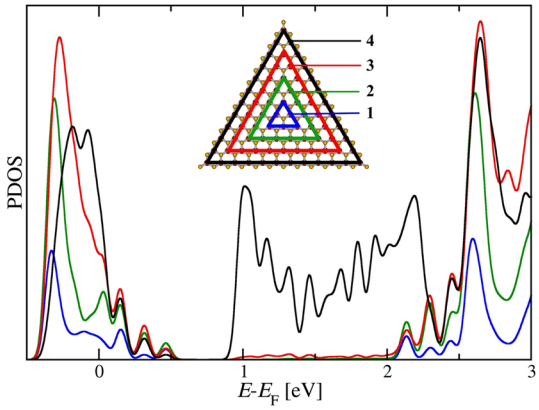

Figure 3. Projected Mo 4d density of states (PDOS) of a $Mo_{78}S_{182}$ nanoflake resulting from groups of Mo atoms triangularly arranged in the nanoflake as indicated in the inset, which also shows the color code.

character of these systems: Although the projected density of states shows that the metal-like states at the Fermi level are basically delocalized over the entire flake, that is, all molybdenum atoms contribute to the band, the absorption in the visible range originates from the edge states. These are located at around 2.2 eV above the Fermi level and originate exclusively from the orbitals located at edge atoms resulting in the absorption peaks of Figure 2. Thus, measurable photoabsorption in the visible range results from energetically high lying edge states, although lower lying metallic states are present.

4. MECHANICAL PROPERTIES OF SINGLE-LAYERED MoS_2 OBTAINED FROM SIMULATED NANOINDENTATION EXPERIMENTS

Mechanical properties of 2D materials can be measured in different ways, for example, by tensile tests or indentation experiments. In these experiments, the material's resistance to mechanical deformation is monitored. Along with experimental measurement, simulations help to understand the individual contributions of atoms and chemical bonds to strength and stiffness of a material. In this and the following part, we will discuss the information that can be obtained from simulations of so-called nanoindentation experiments. In the original experiment, Bertolazzi and co-workers[61] positioned a single layer of MoS_2 on a substrate with prefabricated holes 500 nm in diameter. Thus, the single layer was supported by the circular edge of the hole and self-supporting over it. With an atomic-force microscope, it was possible to press on the self-supporting MoS_2 layer measuring the mechanical resistance of such a single layer.

In this section, we will first discuss the structural and mechanical properties that result from the modeled nanoindentation experiment.[42] The insets of Figure 4 illustrate the experiment by showing the simulation setup: a circular disk with

dx.doi.org/10.1021/ar500318p | Acc. Chem. Res. 2015, 48, 48−55

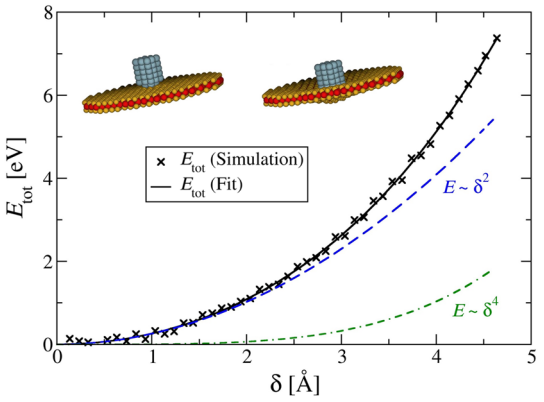

Figure 4. Total energy as a function of deflection. These curves are used as a basis for the calculation of the Young's modulus. The black crosses are the basis for a fit (solid black line) with respect to $E_{tot} = a_0 + a_1\delta^2 + a_2\delta^4$, whose derivative results in eq 1. The dashed lines represent the harmonic (blue) and quartic (green) contributions to the total energy. Inset: Circular MoS_2 layer with fixed edge atoms and a fixed molybdenum tip prior and after indentation. Molybdenum and sulfur atoms of the layer are illustrated as red and yellow spheres, respectively; the tip atoms are represented in blue.

a diameter of 60 Å cut from a single MoS_2 layer was used. The atoms located 4 Å or closer to the edge were fixed, and a tip modeled by 65 molybdenum atoms was successively moved toward the disk. Thereby, short molecular-dynamics simulations with fixed tip structure were performed so that the system could equilibrate to the new tip position.

The structural deformations resulting from the simulated indentation depend on the indentation depth and are also locally different. Elongation and bending of chemical bonds are highest close to the contact point between tip and disk. In contrast, when a biaxial strain is applied to the full layer, the structure is stretched in all in-plane directions leading to an additional global transversal contraction. Here, we observe a locally different contraction with largest values close to the contact point, and also the macroscopic bulging of the disk is highest there.

The energetic and mechanical properties can be derived from an analysis of the changes in energy and applied force, which can be written as[62−65]

$$F = \sigma_0 \pi h \delta + Y\frac{q^3 h}{R^2}\delta^3 \qquad (1)$$

where h is the thickness of the layer, R its radius, δ the deflection, σ_0 the so-called prestrain, and Y the material's Young's modulus,[66] and in our case, the factor q = 1.01 is calculated from the layer's Poisson ratio ν = 0.3.[39,65] A detailed investigation[42,65] of this equation shows that the cubic term includes only the stretching, which applies when the setup's thickness-to-radius ratio is small. The linear contribution to the applied force in eq 1 cannot be attributed to a so-called prestrain[61] originating in van der Waals interactions between the layer and the supporting substrate, because the simulation setup contains only a virtual substrate, that is the clamped boundary conditions. Thus, the linear term may arise from additional deformations, for example, bending, compression perpendicular to the layer, and local displacements caused by the tip.

The indentation simulation gives access first and foremost to the total energy as a function of deflection. By differentiation of the deflection−energy relation, the deflection−force curve given in eq 1 and the mechanical quantities are obtained. The strain σ_0 = 2.6 N/m ("prestrain") seems to depend on the plate size and is in our calculations approximately 80 times larger than the experimental value.[61] The Young's modulus (262 GPa) on the other hand shows excellent agreement with the experimental value (270 GPa[61]) and values obtained for other MoS_2-based materials.[36,39] Additionally the breaking stress, σ_{max}, can be obtained at the fracture point (σ_{max} = 21 GPa;[42] experimental value, 22 GPa[61]), which is defined as the point at which the total energy decreases in comparison to the previous point and at which the gap between occupied and unoccupied orbitals (HOMO−LUMO gap) is closed.

The very good agreement of the results from simulated nanoindentation as well as simulated uniaxial stretching with the experimental data points to the fact that in both processes stretching is the dominant contribution to the deformation. As a consequence, elastic response and mechanical properties can be viewed as comparable in MoS_2 nanotubes and layers. Defects may have only a small effect on Young's modulus and Poisson ratio,[39] but breaking stress and strain are reduced much more significantly. Punctual indented monolayer MoS_2 with defects is estimated to have a comparable robust mechanical behavior in the elastic regime to MoS_2 nanotubes.[42] The mechanical robustness could also be shown in molecular-dynamics simulations of the deformed MoS_2 layer from a point close to piercing, which resulted in the original monolayer structure.

5. ELECTRONIC PROPERTIES OF SINGLE-LAYERED MoS_2 OBTAINED FROM SIMULATED NANOINDENTATION EXPERIMENTS

While the change of the mechanical properties in the indentation experiment is easily accessible, the electronic properties are not. Here, nanoindentation simulations as described in the previous section can help to obtain the system's electronic structure as a function of deflection. Whereas the structural properties vary strongly and locally differently with deflection, the simulations show that the electronic structure of the 2D MoS_2 monolayer is rather robust upon local deformation. Because the nanoindentation setup in the simulated experiment is a finite system, the deformed disks were placed back into a periodic monolayer structure to calculate values for the HOMO−LUMO gap for different deflections (see Figure 5). At first, the gap is influenced

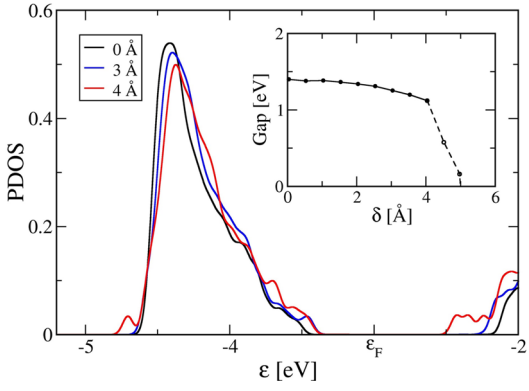

Figure 5. Projected density of states for three different deflections. Inset: band gap as a function of deflection. The dashed line indicates the closing of the band gap by defect states localized at the contact point.

only weakly by the punctual deformation up to a deflection of approximately 4 Å. For larger deflections, midgap states arise due to the beginning destruction of the layer (these are visible, for

dx.doi.org/10.1021/ar500318p | Acc. Chem. Res. 2015, 48, 48−55

example, in the projected density of states that has been calculated for a large circular area around the contact point). The midgap states suddenly close the HOMO−LUMO gap at 5 Å deflection, when the states induced by the local defect dominate the gap. Thus, if a defect is local, the effect on the electronic structure is smaller than that for global deformations, for example, by biaxial stress or indentation by a large periodic blade.[67]

The dependence of the electronic structure's robustness on the defect concentration was shown in a study of quantum transport.[67] Thereby, we could show that electronic transport through an indented MoS_2 monolayer is rather unaffected, only if the defect concentration is small. A global deformation by a periodically repeated broad indentation tip resulted in a much larger conductance drop.

It could be concluded that the local indentation does not influence the transport strongly for large-scale single-layered MoS_2 flakes or quasi-infinite monolayers. The full piercing of a MoS_2 sheet, however, introduced topological defects due to dangling bonds. These result in the occurrence of midgap states and affect the transport properties significantly.[68] Although the defect concentration in these simulated nanoindentation experiments is rather high due to the applied periodic boundary conditions, the minor influence of the defect on the electronic and transport properties leaves MoS_2 monolayers applicable for 2D flexible electronics.

6. ENERGETIC STABILITY OF MoS_2 NANOSTRUCTURES

The fact that MoS_2 exhibits several distinct nanostructural morphologies has already been mentioned in the Introduction, and the insets of most figures in this Account show examples. The most common nanosystems are nanoflakes, quasi-infinite monolayers, nanotubes, fullerene-like structures (nanooctahedra[69,70]), and smaller clusters, in part of Chevrel type. All these structures are accessible by careful choice of experimental conditions; hence it is worthwhile to assess their thermodynamic stabilities by grand canonical considerations and to determine the correlation between the composition and the preferred morphology, specifically with regard to two-dimensional structures. For this purpose, we show the formation energies of several prototypical MoS_2-based species in Figure 6. The dashed lines are motivated by a continuum model, which reflects the change of the total formation energy as a function of the sulfur or molybdenum excess and employs MoS_2, Mo bulk, and the S_8 crown (α-sulfur) as reference structures. In comparison to those reference species, most MoS_2-based nanostructures are stable and quite closely follow the dashed lines that guide the eye in Figure 6.

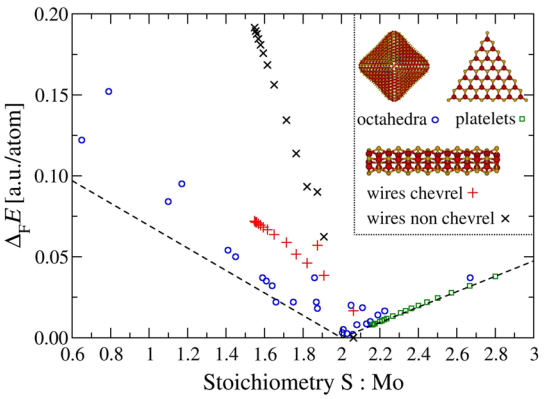

Figure 6. Formation energy, $\Delta_F E$, of prototypical molybdenum sulfide nanostructures as a function of their composition. All formation energies are calculated with respect to the infinitely extended MoS_2 sheet, Mo bulk, and the S_8 crown (α-sulfur) as reference compounds. The dashed lines motivated by a continuum model indicate the energy offset due to the deviation from the ideal MoS_2 stoichiometry.

While the platelet-constructed hollow structures span the whole range of possible stoichiometries due to different sulfur termination schemes along the edges and corners, nanowire-like, ribbon, and nanoflake geometries consist of more well-defined building blocks[6,71] and preferentially contribute to the sulfur-poor (nanowires) or the sulfur-rich (nanoflakes) region of the diagram. Because distinct structural motifs occur in specific regions of the formation energy diagram, Figure 6 indicates that it is thus possible to deliberately choose specific nanostructure geometries by careful choice of the synthesis conditions. The MoS_2-based fullerenes have sulfur-terminated corners, which has been discussed as an origin for catalytic activity. However, as Figure 6 shows, several fullerene-like quasi 0D nanostructures are rather unstable, which could be shown because they are prone to decomposition, starting at the corners, in room-temperature molecular-dynamics simulations.[10,72]

On the other hand, the formation energies of triangular nanoflakes, which are the focus of section 3 of the present discussion, lie nearly on top of the reference line. This is not surprising because they resemble the intact MoS_2 monolayer to a large extent, which is sulfur-terminated at the edges. The sulfur termination is reactive in a similar way as the S_8 crown structure. The edges are, thus, special with respect to optical phenomena as discussed above and to catalytic activity.[1,17] For very small clusters below the wire−flake transition, density-functional calculations and photoelectron spectroscopy data even indicate the presence of sulfur polyanions S_n^{2-} under extremely sulfur-rich formation conditions.[71] Flake geometries are thus also preferable over the wire-like geometries obtained in the sulfur-poor region, which exhibit a complicated crossover from a sulfur-rich to a sulfur-poor termination with increasing cluster length and a concomitant change toward metalloid conductivity in the more extended structures.[6]

7. CONCLUSIONS

The exceptional properties of nanostructures based on molybdenum disulfide have been the focus of this Account. Already from a structural point of view, MoS_2, as other 2D materials, is special: most MoS_2 nanostructures exhibit the bulk topology primarily, either as nanoflakes, nanotubes, or fullerene-like nanooctahedra, where only the edges and corners are structurally different and, thus, the stoichiometry differs slightly from 1:2. Other topologies, as in MoS_2 nanowires, exist as well.

The systematic investigation of the optical absorption spectra of triangular nanoflakes in the visible range revealed a clear red shift due to quantum confinement. The excitation energies in the visible light region agree with the experimental data and show a $1/d^2$ behavior in the Brus equation for $d > 3$ nm. The energy gap discussed in Figure 2 asymptotically converges to the bulk value of 1.9 eV. Although the nanoflakes absorb in the visible range, metallic states at the Fermi level are present. These are delocalized over the entire systems, whereas the absorption in the visible range originates from the higher lying states located at the edge atoms.

To get access to the mechanical properties of MoS_2 monolayers and their influence on structure and electronics,

dx.doi.org/10.1021/ar500318p | Acc. Chem. Res. 2015, 48, 48−55

simulated nanoindentation experiments have been performed based on the original experiment by Bertolazzi and co-workers.[61] Energetics and mechanics have been derived using the theoretical foundations for macroscopic objects.[62−65] Whereas the strain seems to be dependent on the plate size, obtained Young's modulus and breaking stress agree very well with experimental data.

The molecular-dynamics simulations give access to the structural properties as well, which are still inaccessible in experiment: in contrast to applied biaxial stress, deformations are found to be locally different in this experiment, that is, the maximum values of bond elongations, bending, and layer contraction are observed close to the contact point. Moreover, the results support statements that these systems have a robust mechanical behavior and that stretching is the dominating contribution in both local and global deformation, so elastic response and mechanical properties seem to be comparable in MoS_2 nanotubes and monolayers.

Additionally, the material has also very robust electronic properties, especially when it is deformed only locally as in the indentation experiment: The HOMO−LUMO gap is influenced only weakly by indentation up to 4 Å deflection. Further movement of the tip introduces midgap states that close the gap. The closure occurs much later than in a comparable global deformation. Similarly, the quantum transport is influenced only very little by punctual loads. The robustness of MoS_2 monolayers with respect to local deformation makes MoS_2 monolayers a suitable material for flexible electronic applications.

Finally, a comparison of the thermodynamic stability of different MoS_2-based nanostructures revealed a correlation between composition and preferred morphology, particularly for 2D systems. In comparison to chosen reference species, most considered nanostructures were stable. Wire-like, ribbon, and nanoflake structures consist of rather well-defined building blocks and show, thus, either sulfur-rich or sulfur-poor stoichiometries, whereas nanooctahedra do not have a preferential composition. By careful choice of experimental synthesis conditions it is thus possible to deliberately choose specific geometries.

In summary, MoS_2 nanostructures are a unique class of materials with respect to their basic 2D structure, the resulting mechanical behavior especially relating to punctual loads, their edge absorption in triangular nanoflakes, and a correlation between composition and morphology. Thus, these nanostructures are not only special with respect to a single property, but show distinctive features in many areas. A sophisticated use of these attributes resulting in an optimal interplay between them may lay the path to new utilizations. Among these, flexible electronics is only one way, in which the robustness and structural flexibility of MoS_2 is combined with its semiconducting behavior.

AUTHOR INFORMATION

Corresponding Author

*E-mail: Jan-Ole.Joswig@chemie.tu-dresden.de.

Funding

The authors acknowledge financial support by the European Union via ERC Grant INTIF 226639 and the European Regional Development Fund, Project ECEMP-D1 (No. 13857/2379). S.G. gratefully acknowledges start-up funding for her W3 professorship and further support via the International Helmholtz Research School NanoNet, both funded by the Initiative and Networking Funds of the President of the Helmholtz Association.

Notes

The authors declare no competing financial interest.

Biographies

Jan-Ole Joswig received his diploma from the University of Konstanz in 1999 and his Ph.D. degree from the University of Saarland in 2003. After postdoctoral periods at Helsinki University of Technology (Finland) and TU Dresden, he has been a member of the research staff at TU Dresden since 2008.

Tommy Lorenz received his diploma in chemistry from TU Dresden in 2009. He is currently a Ph.D. student at TU Dresden under supervision of Prof. Gotthard Seifert and works at the Helmholtz-Zentrum Dresden-Rossendorf e.V.

Tsegabirhan Berhane Wendumu received his B.Ed. (2007) and M.Sc. (2011) degrees in condensed-matter physics from Mekelle University (Ethiopia). He is currently a Ph.D. student at TU Dresden under the supervision of Prof. Gotthard Seifert.

Sibylle Gemming received her diploma (1993) and Ph.D. (1996) degrees from TU München and a habilitation from TU Chemnitz (2004). She pursued postdoctoral studies at SISSA (Trieste, Italy), UC Santa Barbara (USA), MPI für Metallforschung Stuttgart, and TU Dresden. She is Full Professor of Theoretical Physics at TU Chemnitz and leads a simulation team at Helmholtz-Zentrum Dresden-Rossendorf.

Gotthard Seifert received his diploma in 1975 from TU Dresden and graduated with a Ph.D. in 1979. From 1979 to 1998, he worked as a research assistant and lecturer/professor at the Institute of Theoretical Physics at TU Dresden and got his habilitation in theoretical physics in 1988. He worked as a visiting scientist at SISSA (Trieste, Italy), EPFL (Lausanne, Switzerland), and Forschungszentrum Jülich. After a stay at University of Paderborn, he has held the chair of Theoretical Chemistry at TU Dresden since 2001.

REFERENCES

(1) Gemming, S.; Seifert, G. Nanocrystals: Catalysts on the Edge. *Nat. Nanotechnol.* **2007**, *2*, 21−22.
(2) Fivaz, R.; Moose, E. Mobility of Charge Carriers in Semiconducting. *Phys. Rev.* **1967**, *163*, 743−755.
(3) Wilson, J. A.; Yoffe, A. D. The Transition Metal Dichalcogenides Discussion and Interpretation of the Observed Optical, Electrical and Structural Properties. *Adv. Phys.* **1969**, *18*, 193−335.
(4) Seifert, G.; Tamuliene, J.; Gemming, S. Mo_nS_{2n+x} Clusters - Magic Numbers and Platelets. *Comput. Mater. Sci.* **2006**, *35*, 316−320.
(5) Bertram, N.; Cordes, J.; Kim, Y. D.; Ganteför, G.; Gemming, S.; Seifert, G. Nanoplatelets Made from MoS_2 and WS_2. *Chem. Phys. Lett.* **2006**, *418*, 36−39.
(6) Gemming, S.; Seifert, G.; Bertram, N.; Fischer, T.; Götz, M.; Ganteför, G. One-Dimensional $(Mo_3S_3)_n$ Clusters: Building Blocks of Clusters Materials and Ideal Nanowires for Molecular Electronics. *Chem. Phys. Lett.* **2009**, *474*, 127−131.
(7) Gemming, S.; Tamuliene, J.; Seifert, G.; Bertram, N.; Kim, Y. D.; Ganteför, G. Electronic and Geometric Structures of Mo_xS_y and W_xS_y (x =1, 2, 4; y =1−12) Clusters. *Appl. Phys. A: Mater. Sci. Process.* **2005**, *82*, 161−166.
(8) Enyashin, A. N.; Gemming, S.; Bar-Sadan, M.; Popovitz-Biro, R.; Hong, S. Y.; Prior, Y.; Tenne, R.; Seifert, G. Struktur Und Stabilität von Molybdänsulfid-Fullerenen. *Angew. Chem.* **2007**, *119*, 631−635.
(9) Enyashin, A.; Gemming, S.; Seifert, G. Nanosized Allotropes of Molybdenum Disulfide. *Eur. Phys. J.: Spec. Top.* **2007**, *149*, 103−125.
(10) Bar-Sadan, M.; Enyashin, A. N.; Gemming, S.; Popovitz-Biro, R.; Hong, S. Y.; Prior, Y.; Tenne, R.; Seifert, G. Structure and Stability of

Molybdenum Sulfide Fullerenes. *J. Phys. Chem. B* **2006**, *110*, 25399−25410.
(11) Kibsgaard, J.; Tuxen, A.; Levisen, M.; Laegsgaard, E.; Gemming, S.; Seifert, G.; Lauritsen, J. V.; Besenbacher, F. Atomic-Scale Structure of Mo_6S_6 Nanowires. *Nano Lett.* **2008**, *8*, 3928−3931.
(12) Popov, I.; Gemming, S.; Okano, S.; Ranjan, N.; Seifert, G. Electromechanical Switch Based on Mo_6S_6 Nanowires. *Nano Lett.* **2008**, *8*, 4093−4097.
(13) Gemming, S.; Seifert, G. DFT Investigation of Novel Elongated Molybdenum Sulfide Nanostructures. In *Proceedings of the 19th International Winterschool on Electronic Properties of Novel Materials*; Kuzmany, H., Fink, J., Mehring, M., Roth, S., Eds.; American Institute of Physics: Melville, NY, 2005.
(14) Krause, M.; Mücklich, A.; Zak, A.; Seifert, G.; Gemming, S. High Resolution TEM Study of WS_2 Nanotubes. *Phys. Status Solidi* **2011**, *248*, 2716−2719.
(15) Enyashin, A. N.; Gemming, S.; Seifert, G. Simulation of Inorganic Nanotubes. In *Materials for Tomorrow*; Gemming, S., Schreiber, M., Suck, J.-B., Eds.; Springer: Berlin, Heidelberg, New York, 2007; pp 33−57.
(16) Ivanovskaya, V. V.; Heine, T.; Gemming, S.; Seifert, G. Structure, Stability and Electronic Properties of Composite $Mo_{1-x}Nb_xS_2$ Nanotubes. *Phys. Status Solidi* **2006**, *243*, 1757−1764.
(17) Bollinger, M.; Jacobsen, K.; Nørskov, J. Atomic and Electronic Structure of MoS_2 Nanoparticles. *Phys. Rev. B* **2003**, *67*, No. 085410.
(18) Erdogan, E.; Popov, I. H.; Enyashin, A. N.; Seifert, G. Transport Properties of MoS_2 Nanoribbons: Edge Priority. *Eur. Phys. J. B* **2012**, *85*, 33.
(19) Gemming, S.; Seifert, G.; Vilfan, I. Li Doped Mo_6S_6 Nanowires: Elastic and Electronic Properties. *Phys. Status Solidi* **2006**, *243*, 3320−3324.
(20) Popov, I.; Gemming, S.; Seifert, G. Structural and Electronic Properties of Mo_6S_8 Clusters Deposited on a Au(111) Surface Investigated with Density Functional Theory. *Phys. Rev. B* **2007**, *75*, No. 245436.
(21) Popov, I.; Kunze, T.; Gemming, S.; Seifert, G. Self-Assembly of Mo_6S_8 Clusters on the Au(111) Surface. *Eur. Phys. J. D* **2007**, *45*, 439−446.
(22) Popov, I.; Yang, T.; Berber, S.; Seifert, G.; Tománek, D. Unique Structural and Transport Properties of Molybdenum Chalcohalide Nanowires. *Phys. Rev. Lett.* **2007**, *99*, No. 085503.
(23) Popov, I.; Seifert, G.; Tománek, D. Designing Electrical Contacts to MoS_2 Monolayers: A Computational Study. *Phys. Rev. Lett.* **2012**, *108*, No. 156802.
(24) Joensen, P.; Frindt, R. F.; Morrison, S. R. Single-Layer MoS_2. *Mater. Res. Bull.* **1986**, *21*, 457−461.
(25) Novoselov, K. S.; Jiang, D.; Schedin, F.; Booth, T. J.; Khotkevich, V. V.; Morozov, S. V.; Geim, A. K. Two-Dimensional Atomic Crystals. *Proc. Natl. Acad. Sci. U. S. A.* **2005**, *102*, 10451−10453.
(26) Coleman, J. N.; Lotya, M.; O'Neill, A.; Bergin, S. D.; King, P. J.; Khan, U.; Young, K.; Gaucher, A.; De, S.; Smith, R. J.; Shvets, I. V.; Arora, S. K.; Stanton, G.; Kim, H.-Y.; Lee, K.; Kim, G. T.; Duesberg, G. S.; Hallam, T.; Boland, J. J.; Wang, J. J.; Donegan, J. F.; Grunlan, J. C.; Moriarty, G.; Shmeliov, A.; Nicholls, R. J.; Perkins, J. M.; Grieveson, E. M.; Theuwissen, K.; McComb, D. W.; Nellist, P. D.; Nicolosi, V. Two-Dimensional Nanosheets Produced by Liquid Exfoliation of Layered Materials. *Science* **2011**, *331*, 568−571.
(27) Kam, K. K.; Parkinson, B. A. Detailed Photocurrent Spectroscopy of the Semiconducting Group VIB Transition Metal Dichalcogenides. *J. Phys. Chem.* **1982**, *86*, 463−467.
(28) Lebègue, S.; Klintenberg, M.; Eriksson, O.; Katsnelson, M. Accurate Electronic Band Gap of Pure and Functionalized Graphane from GW Calculations. *Phys. Rev. B* **2009**, *79*, No. 245117.
(29) Splendiani, A.; Sun, L.; Zhang, Y.; Li, T.; Kim, J.; Chim, C.-Y.; Galli, G.; Wang, F. Emerging Photoluminescence in Monolayer MoS_2. *Nano Lett.* **2010**, *10*, 1271−1275.
(30) Mak, K. F.; Lee, C.; Hone, J.; Shan, J.; Heinz, T. F. Atomically Thin MoS_2: A New Direct-Gap Semiconductor. *Phys. Rev. Lett.* **2010**, *105*, No. 136805.
(31) Li, T.; Galli, G. Electronic Properties of MoS_2 Nanoparticles. *J. Phys. Chem. C* **2007**, *111*, 16192−16196.
(32) Radisavljevic, B.; Radenovic, A.; Brivio, J.; Giacometti, V.; Kis, A. Single-Layer MoS_2 Transistors. *Nat. Nanotechnol.* **2011**, *6*, 147−150.
(33) Radisavljevic, B.; Whitwick, M. B.; Kis, A. Correction to Integrated Circuits and Logic Operations Based on Single-Layer MoS_2. *ACS Nano* **2011**, *5*, 9934−9938.
(34) Radisavljevic, B.; Whitwick, M. B.; Kis, A. Small-Signal Amplifier Based on Single-Layer MoS_2. *Appl. Phys. Lett.* **2012**, *101*, No. 043103.
(35) Wang, Q. H.; Kalantar-Zadeh, K.; Kis, A.; Coleman, J. N.; Strano, M. S. Electronics and Optoelectronics of Two-Dimensional Transition Metal Dichalcogenides. *Nat. Nanotechnol.* **2012**, *7*, 699−712.
(36) Kaplan-Ashiri, I.; Cohen, S. R.; Gartsman, K.; Rosentsveig, R.; Seifert, G.; Tenne, R. Mechanical Behavior of Individual WS_2 Nanotubes. *J. Mater. Res.* **2004**, *19*, 454−459.
(37) Kalfon-Cohen, E.; Goldbart, O.; Schreiber, R.; Cohen, S. R.; Barlam, D.; Lorenz, T.; Enyashin, A.; Seifert, G. Radial Compression Studies of WS_2 Nanotubes in the Elastic Regime. *J. Vac. Sci. Technol., B: Nanotechnol. Microelectron.: Mater., Process., Meas., Phenom.* **2011**, *29*, No. 021009.
(38) Kalfon-Cohen, E.; Goldbart, O.; Schreiber, R.; Cohen, S. R.; Barlam, D.; Lorenz, T.; Joswig, J.-O.; Seifert, G. Experimental, Finite Element, and Density-Functional Theory Study of Inorganic Nanotube Compression. *Appl. Phys. Lett.* **2011**, *98*, No. 081908.
(39) Lorenz, T.; Teich, D.; Joswig, J.-O.; Seifert, G. Theoretical Study of the Mechanical Behavior of Individual TiS_2 and MoS_2 Nanotubes. *J. Phys. Chem. C* **2012**, *116*, 11714−11721.
(40) Kaplan-Ashiri, I.; Cohen, S. R.; Gartsman, K.; Ivanovskaya, V.; Heine, T.; Seifert, G.; Wiesel, I.; Wagner, H. D.; Tenne, R. On the Mechanical Behavior of WS_2 Nanotubes under Axial Tension and Compression. *Proc. Natl. Acad. Sci. U. S. A.* **2006**, *103*, 523−528.
(41) Ghorbani-Asl, M.; Borini, S.; Kuc, A.; Heine, T. Strain-Dependent Modulation of Conductivity in Single Layer Transition-Metal Dichalcogenides. *Phys. Rev. B* **2013**, *87*, No. 235434.
(42) Lorenz, T.; Joswig, J.-O.; Seifert, G. Stretching and Breaking of Monolayer MoS_2 - an Atomistic Simulation. *2D Mater.* **2014**, *1*, No. 011007.
(43) Hohenberg, P.; Kohn, W. Inhomogeneous Electron Gas. *Phys. Rev. [Sect] B* **1964**, *136*, B864−B871.
(44) Kohn, W.; Sham, L. J. Self-Consistent Equations Including Exchange and Correlation Effects. *Phys. Rev. [Sect.] A* **1965**, *140*, A1133−A1138.
(45) Porezag, D.; Frauenheim, T.; Köhler, T.; Seifert, G.; Kaschner, R. Construction of Tight-Binding-like Potentials on the Basis off Density-Functional Theory: Application to Carbon. *Phys. Rev. B* **1995**, *51*, 947−957.
(46) Seifert, G.; Porezag, D.; Frauenheim, T. Calculations of Molecules, Clusters, and Solids with a Simplified LCAO-DFT-LDA Scheme. *Int. J. Quantum Chem.* **1996**, *58*, 185−192.
(47) Seifert, G.; Joswig, J.-O. Density-Functional Tight Binding - an Approximate Density-Functional Theory Method. *Wiley Interdiscip. Rev.: Comput. Mol. Sci.* **2012**, *2*, 456−465.
(48) Elstner, M. The SCC-DFTB Method and Its Application to Biological Systems. *Theor. Chem. Acc.* **2005**, *116*, 316−325.
(49) Seifert, G.; Terrones, H.; Terrones, M.; Jungnickel, G.; Frauenheim, T. Structure and Electronic Properties of MoS_2 Nanotubes. *Phys. Rev. Lett.* **2000**, *85*, 146−149.
(50) Niehaus, T. A.; Suhai, S.; Della Sala, F.; Lugli, P.; Elstner, M.; Seifert, G.; Frauenheim, T. Tight-Binding Approach to Time-Dependent Density-Functional Response Theory. *Phys. Rev. B* **2001**, *63*, No. 085108.
(51) Casida, M. E. Time-Dependent Density-Functional Response Theory for Molecules. In *Recent Advances in Density-Functional Theory*; Chong, D. P., Ed.; World Scientific, Singapore, 1995; p 155.
(52) Casida, M. E. Time-Dependent Density-Functional Response Theory of Molecular Systems: Theory, Computational Methods, and Functionals. In *Recent Developments and Applications of Modern Density Functional Theory*; Seminario, J. M., Ed.; Elsevier: Amsterdam, 1996; Vol. *4*, p 391.

(53) Köster, A. M.; Geudtner, G.; Goursot, A.; Heine, T.; Vela, A.; Salahub, D.; Patchkovskii, S. deMon, NRC: Ottawa, Canada, 2004.
(54) Zhechkov, L.; Heine, T.; Patchkovskii, S.; Seifert, G.; Duarte, H. A. An Efficient a Posteriori Treatment for Dispersion Interaction in Density-Functional-Based Tight Binding. *J. Chem. Theory Comput.* **2005**, *1*, 841−847.
(55) Aradi, B.; Hourahine, B.; Frauenheim, T. DFTB+, a Sparse Matrix-Based Implementation of the DFTB Method. *J. Phys. Chem. A* **2007**, *111*, 5678−5684.
(56) DFTB+ http://www.dftb-plus.info.
(57) Wendumu, T.; Seifert, G.; Lorenz, T.; Joswig, J.-O.; Enyashin, A. N. Optical Properties of Triangular Molybdenum Disulfide Nanoflakes. *J. Phys. Chem. Lett.* **2014**, *5*, 3636−3640.
(58) Wilcoxon, J. P.; Newcomer, P. P.; Samara, G. A. Synthesis and Optical Properties of MoS_2 and Isomorphous Nanoclusters in the Quantum Confinement Regime. *J. Appl. Phys.* **1997**, *81*, 7934−7944.
(59) Chikan, V.; Kelley, D. F. Size-Dependent Spectroscopy of MoS_2 Nanoclusters. *J. Phys. Chem. B* **2002**, *106*, 3794−3804.
(60) Brus, L. E. Electron-Electron and Electron-Hole Interactions in Small Semiconductor Crystallites: The Size Dependence of the Lowest Excited Electronic State. *J. Chem. Phys.* **1984**, *80*, 4403−4409.
(61) Bertolazzi, S.; Brivio, J.; Kis, A. Stretching and Breaking of Ultrathin MoS_2. *ACS Nano* **2011**, *5*, 9703−9709.
(62) Föppl, A. *Vorlesungen über Technische Mechanik, Bd. III Festigkeitslehre*; Teubner: Leipzig, 1907.
(63) Hencky, H. Über den Spannungszustand in kreisrunden Platten mit verschwindender Biegesteifigkeit. *Z. Math. Phys.* **1915**, *63*, 311−317.
(64) Schwerin, E. Über Spannungen und Formänderungen kreisringförmiger Membranen. *Z. Technol. Phys.* **1929**, *12*, 651−659.
(65) Komaragiri, U.; Begley, M. R.; Simmonds, J. G. The Mechanical Response of Freestanding Circular Elastic Films Under Point and Pressure Loads. *J. Appl. Mech.* **2005**, *72*, 203.
(66) Lee, C.; Wei, X.; Kysar, J. W.; Hone, J. Measurement of the Elastic Properties and Intrinsic Strength of Monolayer Graphene. *Science* **2008**, *321*, 385−388.
(67) Lorenz, T.; Ghorbani-Asl, M.; Joswig, J.-O.; Heine, T.; Seifert, G. Is MoS_2 a Robust Material for 2D Electronics? *Nanotechnology* **2014**, *25*, No. 445201.
(68) Ghorbani-Asl, M.; Enyashin, A. N.; Kuc, A.; Seifert, G.; Heine, T. Defect-Induced Conductivity Anisotropy in MoS_2 Monolayers. *Phys. Rev. B* **2013**, *88*, No. 245440.
(69) Parilla, P. A.; Dillon, A. C.; Jones, K. M.; Riker, G.; Schulz, D. L.; Ginley, D. S.; Heben, M. J. The First True Inorganic Fullerenes? *Nature* **1999**, *397*, 114.
(70) Parilla, P. A.; Dillon, A. C.; Parkinson, B. A.; Jones, K. M.; Alleman, J.; Riker, G.; Ginley, D. S.; Heben, M. J. Formation of Nanooctahedra in Molybdenum Disulfide and Molybdenum Diselenide Using Pulsed Laser Vaporization. *J. Phys. Chem. B* **2004**, *108*, 6197−6207.
(71) Gemming, S.; Seifert, G.; Götz, M.; Fischer, T.; Ganteför, G. Transition Metal Sulfide Clusters below the Cluster-Platelet Transition: Theory and Experiment. *Phys. Status Solidi* **2010**, *247*, 1069−1076.
(72) Enyashin, A. N.; Gemming, S.; Bar-Sadan, M.; Popovitz-Biro, R.; Hong, S. Y.; Prior, Y.; Tenne, R.; Seifert, G. Structure and Stability of Molybdenum Sulfide Fullerenes. *Angew. Chem., Int. Ed.* **2007**, *46*, 623−627.